NTHAS5: Fifth Korea-Japan Symposium on Nuclear Thermal Hydraulics and Safety
Jeju, Korea, November 26- 29, 2006

NTHAS5-F005

NUMERICAL STUDY ON DISSOLVED GAS AND BUBBLE BEHAVIOR IN FLUID

Eisaku Tatsumi[1*], Takashi Takata[1], and Akira Yamaguchi[1]

[1] Department of Sustainable Energy and Environmental Engineering, Osaka University
Address: 2-1, Yamada-Oka, Suita, Osaka 565-0871, JAPAN, phone: +81-6-6879-7895
E-mail: tatsumi_e@qe.see.eng.osaka-u.ac.jp, takata_t@see.eng.osaka-u.ac.jp and yamaguchi@see.eng.osaka-u.ac.jp

ABSTRACT

In a circulating system of a sodium-cooled fast reactor (SFR), inert gas exists as a dissolved state or a free bubble. The bubbles can cause disturbance in reactivity in the core, nucleation site for boiling and cavitations, flow instability, and influence on heat transfer. Therefore, the investigation of the inert gas behavior is an essential in a design and safety viewpoint. In the present study, we have developed a method for the numerical calculation of the gas behavior in a multi-dimensional flow field and applied the method to the reactor upper plenum. With the present method, one can analyze the bubble behavior of various radii. Mass fractions of the bubbles released at the free surface, dissolved in liquid sodium, and flowing out of the upper plenum are computed. Parametric analyses have been carried out in order to investigate the influence of the bubble size and the flow pattern on the gas behavior. Based on the analyses, we have derived a non-dimensional correlation for the gas behavior and have established a model for the gas transportation in the upper plenum. Application of the model to a system dynamic code of the gas behavior in primary system is a future work.

1. INTRODUCTION

In a sodium-cooled fast reactor (SFR), inert gases exist in the primary coolant system either in a state of dissolved gas or free gas bubbles. There are several sources of the inert gas in the system.

One is argon gas used as a reactor vessel cover gas. The primary coolant system has free surfaces which are covered with the argon gas. The usage of the free surface is unavoidable because reservoir function is needed to absorb the thermal expansion of the liquid sodium. The reactor cover gas is slightly pressurized above the atmospheric pressure. Therefore, the argon gas dissolves in the liquid sodium and is dispersed in the primary coolant system by advection and diffusion. In addition, the free surface is disturbed by the large sodium flow velocity and the sodium flow entrains the argon cover gas. Consequently, free gas bubbles can be included in the liquid sodium by the gas entrainment at the free surface. Another source is helium gas that is produced as a result of disintegration of B_4C control rod material and is emitted as small bubbles in the reactor core.

These free gas bubbles are transported according to the coolant flow in the primary system and may cause disturbance in reactivity in the core, a nucleation site for boiling and cavitation, flow instability, and an influence on heat transfer. Therefore the investigation of inert gas behavior is of importance from the viewpoint of design and safety of the SFR. At the same time, it is necessary to define the acceptance level of the gas content in the primary system because the existence of the gas in the system is unavoidable.

A computational code VIBUL for a dynamics of the gas in the primary system had been originally developed for French fast reactor (Berton, 1991) and modified for Japanese SFR design (Yamaguchi and Hashimoto, 2005). The amounts of free bubbles and dissolved gas in the primary systems and components can be quantified with this code. However, simple models for bubble transport in a plenum are implemented and one-dimensional flow is assumed in the code. The simplification may not be sufficiently accurate to describe the bubble behavior especially in the components such as an upper plenum of the reactor vessel (R/V) and the intermediate heat exchanger (IHX) where multi-dimensional effect is not negligible. It is essential to simulate bubble behavior in the complicated geometry and to estimate the amount of the gas bubbles and dissolved gas. Based on the computation, dominant phenomena to the bubble behavior are identified and the non-dimensional correlations for the bubble transportation are developed. The bubble behavior model currently implemented in the VIBUL code is refined if the new correlations are included to account for the multi-dimensional flow and bubble dynamics.

The objective of the present study is to propose a model of bubble behavior based on theoretical and computational methods. For this purpose, a numerical method for gas bubble transportation has been developed. The computational method is applied to the reactor upper plenum configuration because the flow field in upper plenum is complicated due to internal structure and free surface and the multi-dimensional effect is important. Some bubbles in the reactor upper plenum are conveyed by the sodium flow and emitted at the free surface. Others staying in the plenum may dissolve and disappear in the sodium. The rest of the bubbles in the reactor upper plenum flows out of the outlet nozzle. In the present study, the model of these bubble behavior has been established based on the numerical results.

2. PHYSICAL MODEL

2.1 Flow Field Model

Flow field is computed by solving the governing equations in Eulerian coordinates. The equation of mass conservation is written as:

$$\frac{\partial \rho}{\partial t} + \frac{\partial \rho u_j}{\partial x_j} = 0 \,, \tag{1}$$

where ρ is the density and u_j the j-th component of the velocity vector.

Navier-Stokes equation is represented as:

$$\rho \frac{\partial u_i}{\partial t} = -\frac{\partial \rho u_i u_j}{\partial x_j} - \frac{\partial p}{\partial x_i} + \frac{\partial \tau_{ij}}{\partial x_j} + (\rho - \rho_0) g_i \tag{2}$$

and

$$\tau_{ij} = \mu \left(\frac{\partial u_j}{\partial x_i} + \frac{\partial u_i}{\partial x_j} - \frac{2}{3} \delta_{ij} \frac{\partial u_k}{\partial x_k} \right), \tag{3}$$

where p is the kinetic pressure, g is the acceleration due to gravity, μ is the viscosity coefficient and δ_{ij} is the Kronecker delta function.

Eqs. (1) - (3) are discretized to compute a flow field. Spatial derivatives are approximated by the central difference formula of the second-order accuracy and time integration is performed by the second-order Adams-Bashforth method. SMAC (Simplified Maker and Cell) algorithm is used for calculating the governing equations.

2.2 Mass Conservation of a Single Bubble

A bubble shrinks or grows according to the mass transfer at the bubble-liquid interface. Equations of mass and momentum conservation for a bubble are solved with the Lagrangien scheme. The mass conservation equation for a single bubble is given by:

$$\frac{dN_m}{dt} = -4k\pi r^2 \left[H_c (P + \frac{2\sigma}{r}) - N_d \right], \tag{4}$$

where N_m is moles of gas in a bubble, r is the radius of a bubble, P is the pressure in the liquid sodium, σ is the surface tension and N_d is the molar amount of dissolved gas included in a unit volume of sodium. k is a mass transfer coefficient which is given by:

$$k = \frac{Sh\, D}{2r} \,, \tag{5}$$

where Sh is the Sherwood number and D is the diffusion coefficient of the gas in sodium (Clift et al., 1978). H_c in Eq. (4) is the Henry's constant and is defined as:

$$H_c = \frac{S \rho_{Na}}{M_{Na}} \,, \tag{6}$$

where S is the solubility, ρ_{Na} is the density of sodium and M_{Na} is the molar mass of sodium. The solubility for noble gases such as argon and helium are given by Reed and Dropher (1970). Eq. (4) is solved with the Eulerian explicit method.

2.3 Momentum Conservation of a Single Bubble

A momentum conservation equation with regard to a bubble in a flow field is written as:

$$\frac{d\boldsymbol{V}_G}{dt} = \boldsymbol{g}\left(\frac{\rho_L - \rho_G}{\rho_G}\right) + \frac{3}{8r} C_D \frac{\rho_L}{\rho_G} |\boldsymbol{V}_L - \boldsymbol{V}_G| (\boldsymbol{V}_L - \boldsymbol{V}_G) \,, \tag{7}$$

where $\boldsymbol{V}$, $\boldsymbol{g}$ and C_D are velocity vector, the acceleration vector due to gravity and the drag coefficient. Subscripts G and L indicate gas phase and liquid phase, respectively. The first and the second terms of the right hand side of Eq. (7) are the buoyancy force and the drag force, respectively. The drag coefficient is calculated assuming that a bubble is sphere-shaped. The assumption is valid because the size of the bubble to be considered is small enough and the bubble can be approximated spherical due to high surface tension. Eq. (7) is integrated with the fourth-order Runge-Kutta method.

It is assumed that the influence of a bubble motion on the liquid phase is negligible because the bubble volume fraction is small enough. Hence, one-way-coupling method is used, in which the liquid phase only affects the bubble motion but the influence of the bubble motion on the flow field is ignored. In the present model, the fluid flow and the bubble tracking calculations are performed in a segregated manner; that is, the steady state continuous phase flow field is computed first, then the bubble motion is obtained based on the postulated velocity field.

3. ANALYTICAL CONDITIONS

3.1 Reactor Upper Plenum Modeling

There are several gas sources in the reactor vessel. Gas bubbles circulating in the primary system and emitted from the control rod assemblies are conveyed to the reactor upper plenum from the core. At the free surface of the plenum, argon cover gas is entrained in the liquid sodium as either entrained gas bubbles or dissolved. Therefore, the gas bubble behavior in the upper plenum is important.

Figure 1 shows the cross section of the reactor vessel. The computational region is indicated by the dotted rectangular box in Fig. 1. The domain above the reactor core exit and hot-leg (H/L) inlet nozzle is modeled in two-dimensional Cartesian coordinates. Details of the computational domain are shown in Fig. 2.

In the upper plenum, the dominant coolant flow goes toward the H/L nozzle from the core exit. Some part of the coolant may go upward beyond the upper end of the computational domain.

The 1/10th scaled model water experimental study on flow optimization in the upper plenum of the reactor vessel has been performed (Kimura et al., 2003). From the experiment, it was found that the major flow pattern in the upper plenum was the flow from the core exit directly to the H/L nozzle. In addition, it was observed that coolant rose from the core exit along upper internal structure (UIS) and went downward along H/L pipe after reaching the free surface and finally flowed out of the H/L nozzle. The bubbles conveyed to the near the free surface by the circulating flow are released into the cover gas region because the circulating flow force is weakened and the bubble goes upward by buoyancy. Therefore, we ignore the influence of the circulating flow and assume that all of the bubbles which go beyond the upper end of the computational domain before arriving at the H/L nozzle are released into the cover gas. The simplified model shown in Fig.2 seems to be appropriate from the experimental observation by Kimura et al. (2003).

The configuration data of the computational region are determined based on the 1/10th experimental data. The height between the core exit and the H/L nozzle (H), H/L inner diameter (D_{out}), core exit inner radius (R_{in}), the radius of the reactor vessel ($L1$) and the radial position of the H/L pipe ($L2$) are 0.28m, 0.125m, 0.325m, 0.5m and 0.35m, respectively, as shown in Fig. 3. Equally-spaced mesh divided into 80 (I) × 60 (J) is arranged to the computational region as shown in Fig. 3. Mesh size is 6.25×10^{-3}m and 7.0×10^{-3}m as Δx and Δy,

respectively. This condition is defined as the reference case.

The core exit and the H/L nozzle are treated as the inlet and outlet boundaries in the analyses, respectively. The inlet velocity (core exit) is assumed to be constant in time and uniform in space. The outlet (H/L nozzle) is treated as a constant pressure boundary.

In the experiment, the flow velocity at the core exit was determined based on the Froude number (*Fr*) similarity rule. The *Fr* number is defined as:

$$Fr = \frac{V}{\sqrt{gL}}, \tag{8}$$

where V is the core exit velocity and L is the representative length. The core exit velocity in the experiment was $1/\sqrt{10}$ times smaller than the velocity in the reactor condition, i.e. 1.0m/s. The same outlet boundary condition is used in the present study.

Initial temperature in the upper plenum is the same as the design temperature of the SFR, i.e. 823K. Although the dissolution of the bubbles is related to the system pressure and initial molar concentration of the dissolved gas, atmosphere pressure and no initial dissolution are assumed for simplicity. Also, since the argon gas is the most significant source, the helium gas is not considered.

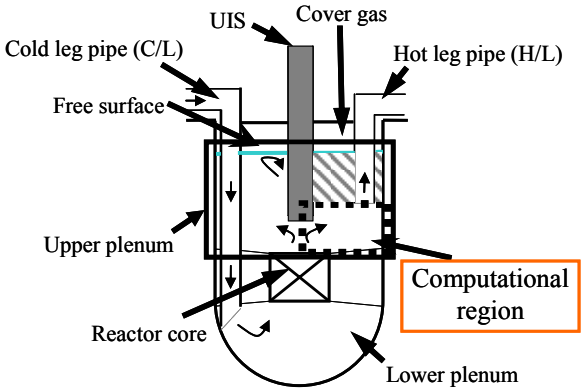

Fig. 1 Cross section of reactor vessel

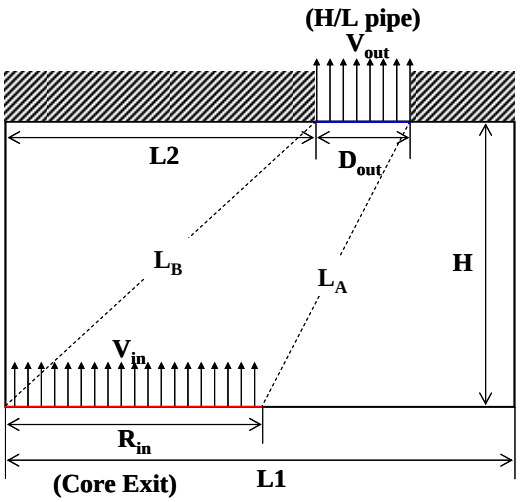

Fig. 2 Computational region

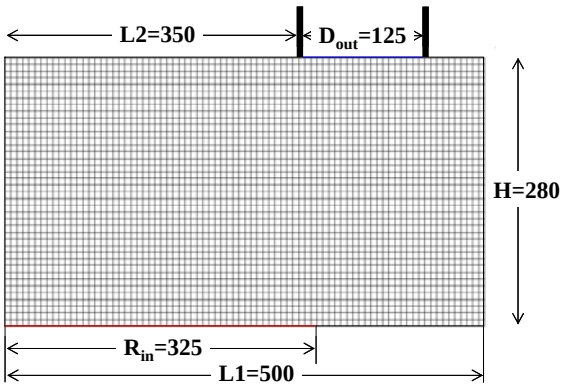

Fig. 3 Computational geometry and mesh arrangement (Reference case)

3.2 Bubbles Conditions

In the numerical analysis, it is necessary to determine maximum and minimum radii to estimate bubble behavior.

When a bubble passes the primary pump or fuel subassemblies where sodium flows at high velocity and turbulence is significant, a large bubble breaks up by the shear force. The shear force is related to the differential velocity at a distance of bubble diameter.

It is known that a bubble breaks up in a flow field when the Weber number (*We*) is greater than the critical Weber number (We_c) of 4.7 (Lewis and Davidson, 1982). *We* is expressed as:

$$We = \frac{2r\rho\overline{u'^2}}{\sigma}, \tag{9}$$

where $\overline{u'^2}$ is the mean square of the flow velocity fluctuation within the geometrical scale of the bubble diameter. Because it is difficult to evaluate the $\overline{u'^2}$, a methodology was proposed to estimate the critical radius for the bubble breakup based on the energy dissipation rate in the components (Lewis and Davidson, 1982). The maximum stable radius is given by:

$$r_m = 0.835\sigma^{0.6}\varepsilon^{-0.4}\rho^{-0.2}, \tag{10}$$

where ε is the energy dissipation per unit volume. Regarding the primary pump, the energy dissipation is estimated from the pump hydraulic efficiency which corresponds to the turbulence energy dissipation. The energy dissipation is calculated to be 9.77×10^5 W/m^3 and then the maximum radius is easily given from Eq. (10) to be 297μm disintegration in the Super Phenix design condition. Since a bubble density is thin in the primary cooling system, bubble coalescence is negligible. Therefore, a bubble larger than 297μm in radius does not exist in the system.

The inner pressure of a bubble increases significantly due to surface tension in accordance with the decrease of bubble radius. Consequently, a tiny bubble dissolves immediately.

In the previous study of the gas dynamics analysis (Yamaguchi and Hashimoto, 2005), it was found that most of the bubbles existed in the range of 10 - 80μm. Hence we select 1μm and 100μm as the minimum and the maximum radii, respectively.

The bubble radius is discretized logarithmically into 50 groups ranging from 10^{-6}m to 10^{-4}m. A bubble is placed for each computational mesh at the inlet boundary. Therefore 52 bubbles from each of radius groups are placed at equal intervals in each computation (in total, 2600 bubbles in one case).

3.3 Parametric Analysis

A parametric analysis is performed in order to estimate the influence of the plenum geometry and flow field on the bubble behavior. We select the following parameters: the height between the core exit and the H/L nozzle (H), the radial position of the H/L pipe ($L2$), the H/L inner diameter (D_{out}) and the core exit velocity (V_{in}). H, $L2$ and D_{out} are the parameters that characterize the shape of the plenum, and V_{in} represents the fluid inertia force. We investigate the influence of the flow field on the gas behavior in these parametric studies. Each parameter is varied as displayed in Table 1. From the parametric analysis, the correlation for the gas behavior is to be established.

Table 1 Selection parameter value for the sensitivity analysis

parameter				**Reference Case**			
H		210mm	245mm	**280mm**	315mm	350mm	
$L2$		250mm	275mm	**300mm**	325mm	350mm	
D_{out}	50mm	75mm	100mm	**125mm**	150mm	175mm	
V_{in}	0.4m/s	0.6m/s	0.8m/s	**1.0m/s**	1.2m/s	1.4m/s	1.6m/s

4. RESULTS AND DISCUSSIONS

4.1 Results of Flow Field and Bubble Behavior Analysis

Figure 4 shows the stream lines of the flow velocity. The color contour represents the magnitude of the velocity. The flow field can be explained from this figure. Liquid sodium flows into the upper plenum from the reactor core and then flows out of the H/L pipe. A large circulation is observed in the bottom-right corner in Fig. 4.

Bubbles are placed on the inlet boundary at equal interval and then the bubble behavior is computed by solving Eq. (4) and Eq. (7). The mass fractions of the bubbles released at the free surface f_{rel}, dissolved in liquid sodium f_{dis} and flowing out of the upper plenum f_{out} are calculated. The three quantities sum up to unity. Figure 5 shows the fractions as a function of the bubble radius.

In Fig. 5, it is seen that the dissolution fraction is the largest for small bubbles, and the outflow fraction becomes most significant for bubbles larger than 2μm. The surface tension becomes dominant as the bubble radius decreases. The smaller bubbles have the higher dissolution fraction due to the high surface tension and hence the dissolution fraction (f_{dis}) increases. On the contrary, in case of larger bubbles, the drag force becomes dominant. The bubbles are transported from the core exit to H/L nozzle according to the flow field. Therefore, the outflow fraction becomes the largest.

It is found that the fractions are almost constant for the bubbles larger than a certain radius that is to say 10^{-5}m. The terminal velocity of 100μm bubble calculated to be 3.62×10^{-2}m/s and is much smaller than the core exit velocity. Consequently, it might be said that the influence of the buoyancy force on the bubble behavior does not work compared with that of the inertia force. As a result, almost constant fractions are obtained regardless to the radius, when the f_{dis} becomes zero.

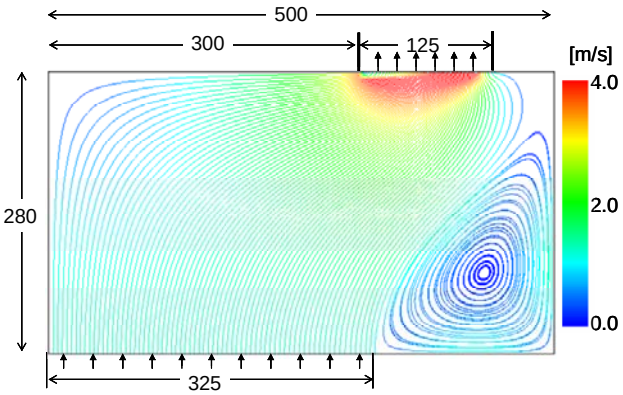

Fig. 4 Stream line in reference case

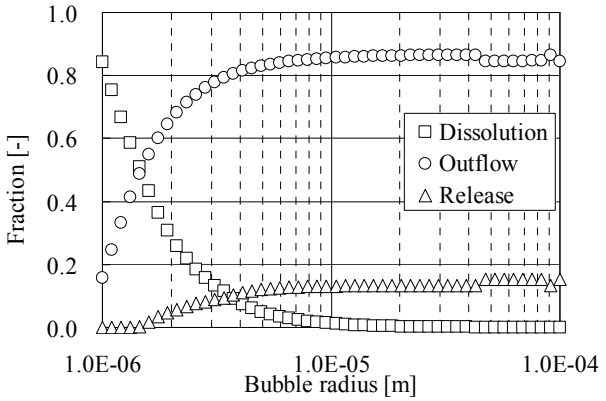

Fig. 5 Bubble behavior in reference case

The bubble behavior shown in Fig. 5 is influenced by the geometry of the plenum and flow field. Among the parameters, it is found that the plenum height H, which is distance between inlet and free surface, have a significant effect on f_{rel}, f_{dis} and f_{out}. Figures 6 - 8 show the mass fractions for different plenum height as a function of the bubble radius.

The dissolution fraction f_{dis} increases as H becomes large as shown in Fig. 6. This is attributed to the fact that the bubbles tend to stay for long time in the plenum.

The outflow fraction f_{out} becomes smaller as H becomes large as shown in Fig. 7. As H increases, the horizontal flow velocity reduces and the drag force to a bubble is weakened in the lateral direction. Hence, the bubble flowed into upper plenum goes upward and does not reach to the H/L pipe.

The release fraction f_{rel} shows a different tendency with regard to the bubble size. In case of the smaller bubbles, f_{rel} becomes smaller as H increases. On the contrary, in case of larger bubbles, f_{rel} becomes larger as H increases. Because the smaller bubble has high dissolution fraction and completely dissolved before it reaches at the free surface, the release fraction becomes smaller as H increases. In case of larger bubble, as H becomes larger, the horizontal drag force to a bubble is weakened due to decrease of the horizontal flow velocity. Also, the bubble goes upward according to the buoyancy. Therefore, the release fraction comes up as H becomes large.

In addition, it is found that the release fraction increases abruptly at about 50μm of bubble radius, as shown in Fig. 8. In the present analysis, 52 bubbles behavior are tracked per one radius group. The release fraction can increase or decrease at about $1/52 \approx 1.9\%$ when one bubble of 52 bubbles is released or not to the cover gas. Hence, the release fraction is abruptly fluctuated.

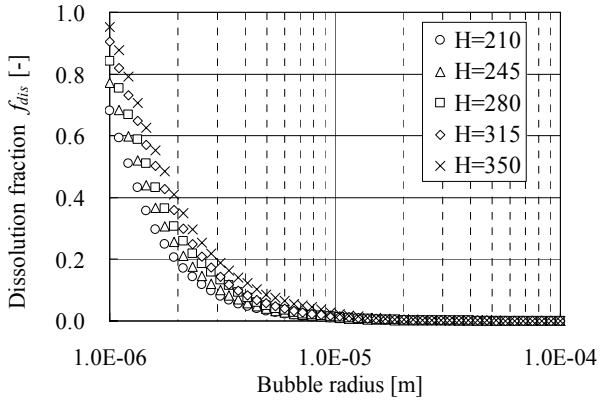

Fig. 6 Influence of height on dissolution fraction

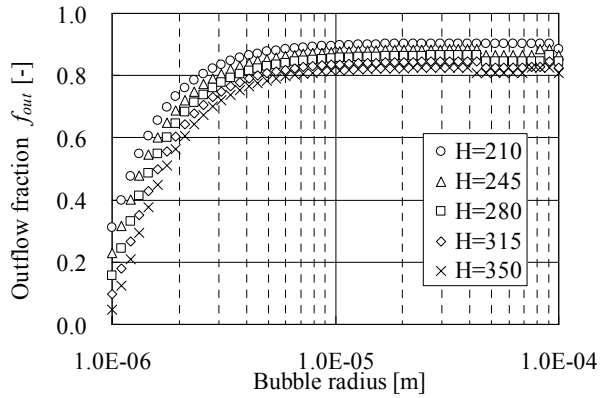

Fig. 7 Influence of height on outflow fraction

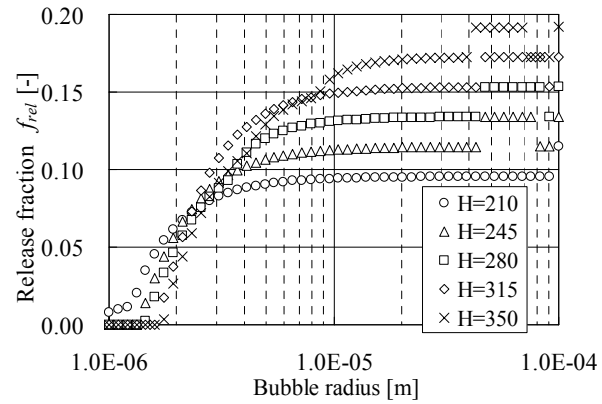

Fig. 8 Influence of height on release fraction

4.2 Dimensionless Numbers for Gas Behavior Model

VIBUL code has been developed for a dynamics of the gas behavior in the primary system. It employs simple models about the bubble behavior in the coolant system as described in the following. In the upper plenum, the model of bubbles released at the free surface is represented with the hydraulic diameter of the free surface in the upper plenum L_{Na}, horizontal velocity at the free surface v_h, the area of the free surface S_{Na}, the volume of the sodium in the plenum V_{Na} and the terminal rising velocity of a bubble v_t. It is assumed that a bubble flowing into upper plenum is transported at horizontal velocity v_h and vertical velocity v_t. t_h is the time transported horizontally from the inlet to the outlet in the upper plenum and is given by:

$$t_h = \frac{L_{Na}}{v_h}. \tag{11}$$

t_t is the time reaching to the free surface and is given by:

$$t_t = \frac{V_{Na}}{S_{Na} v_t}. \tag{12}$$

It is assumed for simplicity that the bubble in the upper plenum is released from the free surface if t_h is greater than t_t, and is transported to outlet nozzle if t_h is less than t_t.

From a result of the reference case analysis, it is found that the advection and dissolution are dominant phenomena that control the bubble behavior in the plenum. For consideration of multi-dimensional effects on the bubble behavior, we propose an empirical model of the bubble behavior in the upper plenum derived from a numerical experiment. Dimensionless numbers which represent the balance of the forces regarding a bubble and a flow field are used for the modeling of the bubble behavior.

It is considered that Froude number and Reynolds number are the key dimensionless numbers to express the flow phenomenon. Froude number (*Fr*) is defined as:

$$Fr = \frac{V_{in}}{\sqrt{gH}}, \tag{13}$$

Reynolds number (*Re*) is defined as:

$$Re = \frac{\rho V_{in} R_{out}}{\mu}, \tag{14}$$

where R_{out} is the core exit inner radius and μ is the viscosity coefficient.

Eötvös number (*Eo*) and Froude number (*Fr'*) relating to the terminal velocity of a single bubble are important to express the property of the bubble. Eötvös number is the ratio of the buoyancy to the surface tension. Eötvös number is defined as:

$$Eo = \frac{g(\rho_L - \rho_G) d^2}{\sigma}, \tag{15}$$

where *d* is the diameter of the bubble.

Fr' denotes the ratio of the inertia force of a bubble to the gravity force. *Fr'* is defined as:

$$Fr' = \frac{V_t}{\sqrt{gL'}}. \tag{16}$$

The terminal velocity V_t is used for representation of the inertia force of a bubble. *L'* is the average value of L_A and L_B shown in Fig. 2.

$$L' = (L_A + L_B)/2. \tag{17}$$

We derive a correlation for bubble behavior using the dimensionless number mentioned above, i.e. two Froude numbers in term of fluid flow and bubble motion, and Eötvös number.

4.3 Derivation of Non-dimensional Correlation for Gas Behavior

f_{dis} and f_{out} evaluated for the computational cases shown in Table 1 are summarized in Figs. 9 and 10. These figures show

that f_{dis} and f_{out} have widely scattered. It seems no distinct relationship is obtained in terms of the bubble radius. Thus, correlation to express f_{dis} and f_{out} as a function of dimensionless numbers are developed in the following.

Dimensionless numbers used in the present study are *Fr*, *Fr'* and *Eo*. *Fr* denotes the ratio of fluid inertia force to fluid gravity force. It is emphasized that *Fr'* is a dimensionless number with regard to a bubble motion. In other words, the bubble velocity is used in Eq. (16) and *Fr'* characterize the inertia force of a bubble. Accordingly, the inertia force of the fluid flow and bubble motion and the gravity force are related by $Fr\,Fr'$.

Eo number denotes the ratio of buoyancy acting on a bubble to surface tension of a single bubble. The relationship of the buoyancy, surface tension, fluid inertia force and fluid gravity force acting on a single bubble is represented by a function of *Fr'* and *Eo*.

f_{dis} is reduced by a dimensionless formula as a function of $Fr\,Fr'^{1.5}\,Eo^{-0.5}$. The function of the correlation is expressed as:

$$f_{dis} = 2.995\times10^{-5}(Fr\,Fr'^{1.5}\,Eo^{-0.5})^{-0.9108}, \qquad R^2 = 0.9963, \tag{18}$$

where R^2 is correlation coefficient. If f_{dis} calculated in Eq. (18) is greater than one, it is assumed one is substituted for f_{dis}.

The non-dimensional correlation for f_{out} is also derived in a similar way of f_{dis}. A function as $(H / D_{out})^{0.2}$ is multiplied f_{out} in all case computed in parametric analysis because the effect of D_{out} and H on f_{out} is large. The correlation between f_{out} $(H / D_{out})^{0.2}$ and $Fr\,Fr'^{1.5}\,Eo^{-0.5}$ is shown in Fig. 12. It is found that f_{out} can be expressed by dimensionless numbers and all the computational results are fitted on a single curve. The function of the approximated curve is described as:

$$f_{out} = (D_{out}/H)^{0.2}\left\{1-4.200\times10^{-9}\exp(-1.035X^2-11.59X-12.96)\right\}, \qquad R^2 = 0.9930, \tag{19}$$

$$X = \log(Fr\,Fr'^{1.5}\,Eo^{-0.5}). \tag{20}$$

If f_{out} calculated in Eq. (19) is less than zero, it is assumed that zero is substitute for f_{out}.

We have established the non-dimensional correlation function for f_{dis} and f_{out}. It is matter of course that f_{rel} can be calculated from the others. We have proposed the model of bubble behavior in the upper plenum using the dimensionless correlations which takes multi-dimensional effect on bubble into consideration. It can be seen that the numerical results are excellently expressed as shown in Figs. 11 and 12.

Although the computational results are scattered as shown in Fig. 9, the proposed correlation function is converted with all the date as in Fig. 11.

5. CONCLUSIONS

We have carried out the analysis of the fluid flow and gas bubble behavior in the reactor upper plenum coupled with multi-dimensional flow field. The flow field in the upper plenum is complicated due to internal structure and free surface and the multi-dimensional effect is important.

As a result of the analyses, it is found that the bubble behavior depends on the bubble radius and the flow field. Parametric analyses are carried out in order to evaluate the influence of the flow field on the bubble behavior. Based on the parametric analyses, mass fraction of the bubbles released at

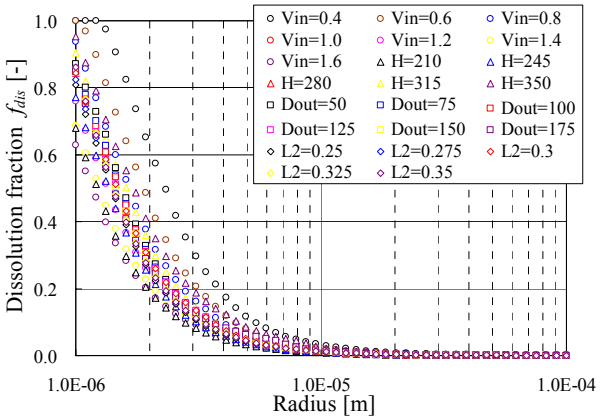

Fig. 9 Dissolution fraction in parametric study

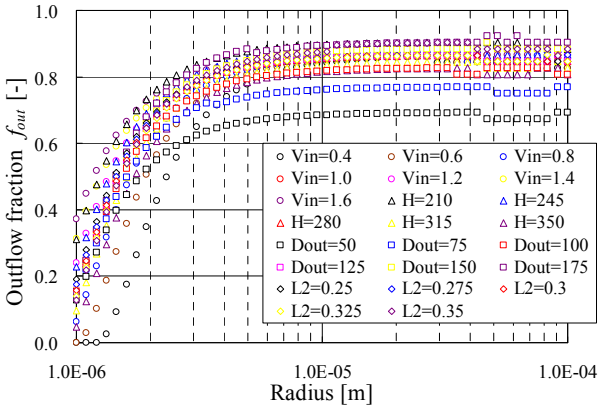

Fig. 10 Outflow fraction in parametric study

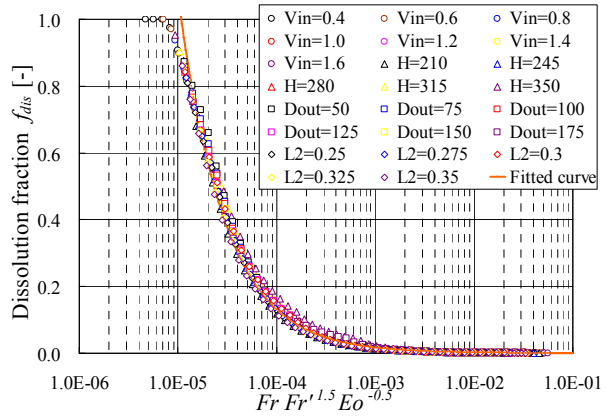

Fig. 11 Non-dimensional correlation for dissolution fraction

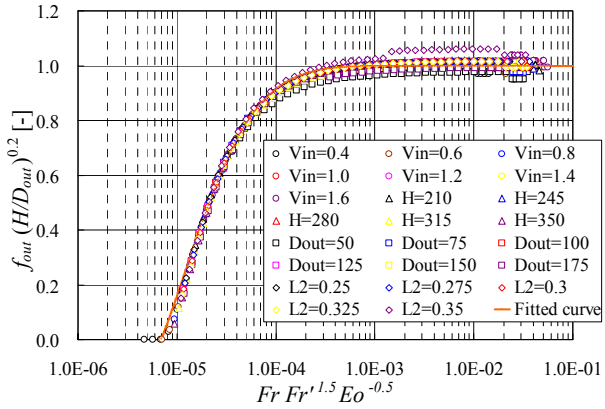

Fig. 12 Non-dimensional correlation for outflow fraction

the free surface (f_{rel}), dissolved in liquid sodium (f_{dis}) and flowing out of the upper plenum (f_{out}) are quantitatively evaluated. We have derived correlations for f_{dis}, f_{out} and f_{rel} using dimensionless numbers; *Fr*, *Fr'* and *Eo* number.

The new physical model is proposed of the gas behavior in the upper plenum which takes multi-dimensional effects on gas behavior into consideration.

Future work is the application of the model to a system dynamics of the gas behavior in the primary system. The acceptance level of the gas content in the primary system is to be determined using the VIBUL code, for example.

NOMENCLATURE

C_D	Drag coefficient
D	Diffusion coefficient
D_{out}	H/L inner diameter [m]
d	Diameter [m]
Eo	Eötvös number
Fr	Froude number
Fr'	Froude number relating to terminal velocity of a single bubble
g	Acceleration due to gravity [m/s^2]
H	Height between core exit and H/L nozzle [m]
H_c	Henry's constant [mol/s/Pa]
k	Mass transfer coefficient [m/s]
L	Length [m]
L_{Na}	Hydraulic diameter of free surface in upper plenum [m]
$L2$	Radial length of H/L nozzle [m]
M_{Na}	Molar mass of sodium [kg]
N_d	Molar amount of a dissolved gas included in a unit volume of sodium [mol/m^3]
N_m	Molar amount of a gas in a bubble [mol]
p	Kinetic pressure [Pa]
P	Pressure [Pa]
r	Radius [m]
S	Solubility [Pa^{-1}]
Sh	Sherwood number
S_{Na}	Area of free surface in upper plenum [m^2]
u_j	i direction velocity component [m/s]
V	Velocity [m/s]
V_{in}	Inlet velocity [m/s]
V_{Na}	Volume of sodium in upper plenum [m^3]
V_t	Terminal velocity of a bubble [m/s]
v_h	Horizontal velocity at free surface in upper plenum [m/s]
v_t	Terminal velocity of a bubble [m/s]
We	Weber number

Greek Letters

δ_{ij}	Kronecker delta function
μ	Viscosity coefficient [kg/m/s]
ρ	Density [kg/m^3]
σ	Surface tension [N/m]

Subscripts

G	Gas phase
L	Liquid phase

REFERENCES

Berton, J. L., VIBUL (1991). "Un modèle de calcul de la voe des bulles en réacteur," NTCEA, SSAE, LSMI91, 023.

Clift, R., Grace, J. R. and Weber, M. E. (1978). "Bubbles, drops, and particles," *Academic Press*

Kimura, N., Hayashi, K. et al. (2003). "Hydraulic Experiment for Compact Reactor Vessel –Measurement of Flow Field Optimization in Upper Plenum," JNC TN9400 2003-032

Lewis, D. A. and Davidson, J.F. (1982). "Bubble splitting in Shear flow," *Trans. IChemE*, Vol. 60, pp. 283-291.

Reed, E. L. and Dropher, J. J. (1970). "Solubility and Diffusivity of inert gases in liquid sodium, potassium and NaK," *Liquid Metal Engineering Center Report* LMEC-69-36

Yamaguchi, A. and Hashimoto, A. (2005). "A Computational Model for Dissolved Gas and Bubble Behavior in the Primary Coolant System of Sodium-Cooled Fast Reactor," 11th International Topical Meeting on Nuclear Reactor Thermal-Hydraulics, France, October, 2005, 477